Enhanced Rescue Lift Capability

Larry A. Young
Aeromechanics Branch
Flight Vehicle Research and Technology Division
NASA Ames Research Center
Moffett Field, CA 94035

Abstract

The evolving and ever-increasing demands of emergency response and disaster relief support provided by rotorcraft dictate, among other things, the development of enhanced rescue lift capability for these platforms. This preliminary analysis is first-order in nature but provides considerable insight into some of the challenges inherent in trying to effect rescue using a unique form of robotic rescue device deployed and operated from rotary-wing aerial platforms.

Nomenclature

C_T	Helicopter main rotor thrust coefficient
$\vec{i}_*, \vec{j}_*, \vec{k}_*$	Global Cartesian coordinates; positive right, positive forward, and positive up, respectively
k	Empirical rotor wake induced inflow constant
r/R	Radial distance from the rotor axis, as the origin, nondimensionalized by the rotor radius
R	Helicopter main rotor radius, m
T_i	Thrust from the ith thruster (ducted-fan, or cold-gas- or air-jet, etc.)
T_R	Helicopter rotor thrust
$\vec{v}_R$	Rotor wake velocities; positive downward
W	"Vectored" hoist payload weight
x	Lateral displacement with respect to hub location (origin)
y	Longitudinal displacement with respect to hub location (origin)
z	Vertical displacement with respect to hub location (positive up)
x_o, y_o, z_o	Cartesian coordinates, relative to rotor hub center, of hoist "fixed-end" pivot
Ω	Helicopter main rotor rotational speed, radians/s
χ	Fraction of hoist cable length exposed to the rotor wake
ε	Relative angle of thrust/thruster with respect to hoist axis
γ	Actuator disk distributed circulation strength, $\gamma = \sqrt{2C_T}\Omega R$
Γ	Rotor blade-root vortex circulation strength, $\Gamma = 2\pi C_T \Omega R^2$

Introduction

USE of helicopters for emergency response and disaster relief has been a hallmark of their application from nearly the very moment of their practical realization. In particular, the use of helicopters for rescue lift operations has been a key capability for these aircraft. Since the first rescue lift (Ref. 1), the helicopter has been called almost innumerable times to provide aid and rescue those in need from natural and man-made disasters (Fig. 1). Increasingly, though, greater demands are being placed upon aviation assets and aircrews to respond to both natural and manmade disasters.

Presented at the 63rd Annual Forum of the AHS International, Virginia Beach, VA, May 1-3, 2007.

Fig. 1 -- Helicopters in Disaster Relief
(Image Courtesy of the US Coast Guard)

Despite these long-standing successes in vertical lift rescue, there are several areas where rescue capability can be enhanced by advanced technology. Table 1 summarizes some of these areas and the possible technological advances that might be of utility. Several of these notional enhanced disaster relief and emergency response capabilities are taken from Ref. 2. The first capability listed, "rescue lift," is the one explored in some depth in this paper.

Table 1 – Need for Enhanced Rescue Capability

Enhanced Capability	Technologies of Possible Utility
Rescue lift from heretofore inaccessible sites and/or under severe conditions	Ducted-fan vehicle design concepts; robotics, including effectors design; advanced control theory; human-system interfaces; helicopter slung load dynamic analysis
Networks of automated "disaster relief" stations	Automation and intelligent system design; robotics
Robotic rescue devices providing services and responsiveness beyond first-responder physical limitations and available onsite expertise/equipment	Robotics; networked intelligent systems; human-system interaction; system integration (e.g. "plug and play" architectures)
Optionally piloted aerial assets for extreme and/or expendable missions	Automation & intelligent system design; advanced flight control concepts; advanced situational awareness sensors
Improved first-responder mobility (both aerial and surface mobility) in disaster stricken areas	Aeromechanics and advanced vehicle design and analysis; mission simulation tools
Unconventional autonomous aerial vehicle designs supporting disaster relief missions	Aeromechanics and advanced vehicle design and analysis; mission simulation tools

Several emerging technologies now present an opportunity to consider new approaches to enhancing rotorcraft rescue lift capability. Among these new technologies are advances in robotics and automation as well as complementary advances in vehicle design and aeromechanics of small autonomous vertical lift platforms. A perhaps unanticipated fusion of these technologies can lead to novel concepts for robotic rescue devices that can be incorporated as an integral part of future rotorcraft rescue operations. One such robotic rescue device concept will be the principal topic of this paper.

Figure 2 illustrates the "vectored" rescue hoist concept. Conventional helicopter rescue hoists significantly limit operational flexibility to performing lifts in relatively obstacle free environments directly below the rotor disk "footprint" of the helicopter. To attempt otherwise is to run the risk of snagging the hoist cable on intervening obstacles or even, in certain cases, risking blade strike with large superstructures or coastline cliffs and other rock formations the helicopter may be flying alongside. What is required is an additional element of control (beyond that afforded by the pilot station keeping with the helicopter) in terms of positioning the hoist sling/basket -- both in terms of precision and overall magnitude of lateral/radial displacement from directly underneath the helicopter. This enhanced control of the hoist "free end" would be effected by a specialized teleoperated hoist sling/basket-module that would have mounted to it multiple ducted-fan propulsors whose combination of thrust vector lines of action would displace the sling/basket to the required offset from the aircraft. The "vectored" teleoperated hoist module would be controlled by the hoist lift operator onboard the aircraft.

A "vectored" hoist would have enough ducted-fan propulsor thrust capability to move an unloaded sling/basket into a needed lateral position for rescue -- but not when carrying a victim. Therefore, it is anticipated that in one possible mode of operation the "vectored" rescue hoist module would also be outfitted with a reel of guide line that would be secured, by those needing rescue, to allow motorized "rappelling." This motorized guideline would then be used to move the hoist sling/basket (with victim) downward and sideward along a diagonal line -- from an otherwise inaccessible pickup location the helicopter couldn't fly alongside or over – to position it directly

underneath the helicopter for optimum lifting once clear of hazardous obstacles.

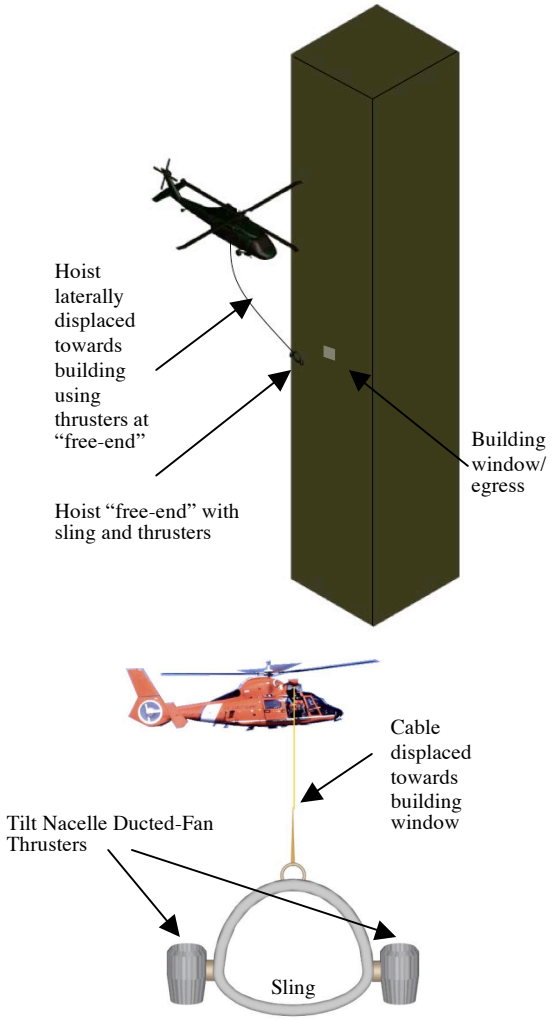

Fig. 2 – "Vectored" Rescue Hoist: (a) deploying hoist near building and (b) perspective view (from building window/egress viewpoint)

By way of comparison, Table 2 summarizes some of the other concepts that have been suggested in the literature for enhancements to current capabilities in rescue vertical lift capability. It must be stressed that Table 2 is not intended to be a comprehensive survey of all concepts proposed for helicopter-enabled rescue devices; nor does it imply or disabuse the feasibility of the cited concepts. The Table 2 concepts range from passive structures appended/mounted to helicopter, to various actively deployed/telescoping structures and booms, all the way to aerodynamically controlled/maneuvered platforms. All of the proposed rescue devices noted in Table 2 have their assorted challenges in realizing practical implementation. There is, in all these concepts, a common thread: a sought after capacity for extending the reach of helicopter rescue lift beyond the confines described by the main rotor radius. The increasing demands of modern civilization as to improvements in disaster relief and emergency response efforts will be a major impetus to arrive at satisfactory design solutions for this problem of enhanced helicopter rescue lift.

Table 2 – Summary of Some Previously Proposed Helicopter Rescue Lift Concepts

Concepts:
1. Telescoping helicopter rescue boom with safety line/reel with tension-release clips (Ref. 3); lightweight system that minimizes the influence of downwash on recovery victims; still requires a vertical lift of victim, where such lift could only be effected by pendulum-like swinging of the victim from pick-up point to lift point.
2. Rigid truss/bridge-like cantilevered structures appended, upon need, to helicopter airframe (Ref. 4); chief advantage is conceptual simplicity in terms of no moving structures required; chief disadvantages are potential structural modifications to mount on airframe, significant effort and time required to mount, and limited ability to counterbalance large vehicle moments stemming from center-of-gravity offsets and forward-flight aerodynamic loads.
3. Deployable telescoping truss/bridge-like structures with appropriate telescoping counterweight to balance center-of-gravity and deployment moments (Refs. 5, 6, and 7); chief advantage is that the concept theoretically provides for "walk-on" of victims onto rescue platform; chief disadvantages of concept are mechanical complexity; potential of system failures where the truss structure fails to retract, issues on how to maintain "positive" contact with pick-up point, and many of the same installation concerns note with the rigid truss systems noted above.
4. Suspended/slung-load rescue basket/hoist wherein large lateral displacements and station-keeping away from directly underneath the helicopter is effected by movable aerodynamic vanes operating in the direct downwash of the helicopter (Ref. 8); advantage of concept is its ability to effect rescue lift laterally displaced from directly underneath the helicopter; its chief disadvantage is that the rescue basket/hoist (and victim) still have to be underneath the rotor disk (so as to be within the rotor wake downwash)
5. Wall-climbing platform (with propeller/rotary-wing enabled propulsion/mobility, Ref. 9); chief advantage is that it allows for rescue/access from the building exterior along the outer walls; chief disadvantages are issues related to deployment, traversing uneven surfaces along the building exterior, and in general maintaining with certainty adequate surface contact and stability for access/egress by people onto and off the platform.
6. Large rescue platforms suspended/slung-loaded from helicopter with lateral displacement effected by an array of ducted fans (Ref. 10); concept is similar to, though much larger than the "vectored" rescue hoist studied in this paper; chief advantage is the concept's capacity for carrying large number of victims; additionally multiple cables/winches allow for platform to be kept at a relatively benign orientation for "walk-on" rescue; chief disadvantage of the concept is it size and complexity.

For the vectored rescue hoist concept to find realization, the inherent added system and operational complexity of the concept must be matched by a substantial improvement in rescue capability in order to justify this effort. In effect, this, and similar, robotic rescue devices must enable the ability to "reach the previously unreachable" in terms of effecting rescue in order to one day see operational usage.

Concept of Operations

Table 3 summarizes some of the various types of rescue missions that could be expedited by the vectored rescue hoist concept or derivatives, thereof. This paper will primarily focus on one rescue mission, that of rescue from the windows or exterior walls of high-rise buildings. Despite this focus, vectored rescue hoists are not a "one mission" type of concept.

Table 3 – Types of Recovery

Direct Recovery: Primary function is to act as a hoist (albeit with lateral displacement capability) to recover, or rescue, people in need of emergency attention or located in a hazardous or physically untenable location.
1. Rescue from windows, ledges, and exterior walls of high-rise buildings
2. Rescue from (highly congested, cluttered, or otherwise inaccessible to direct vertical lift) high-rise building tops
3. Rescue from shear cliff faces, with overhang, escarpments, that prohibit direct vertical lift
4. Maritime rescue from (highly congested. cluttered, swaying/shifting, or otherwise inaccessible to direct vertical lift) ship decks
Deployment of Rescue Supplies and Devices: To provide a means of deploying supplies, (robotic) devices, and other equipment from rotary-wing platforms to physical locations unreachable with other delivery schemes.
1. Lowering by hoist/slung-load and deploying ground-based mobile search and rescue robotic devices.
2. Deploying specialized sensors, two-way communication systems, beacons, RFID or visual markers, and specialized aid kits with telemedicine capabilities.
3. Robotic mobile "guide dogs" and stationary "guides" for mapping, identifying, and communicating locations of cleared pathways and egress points to both rescue teams and people attempting to self-extricate themselves from disaster sites (e.g. trying to leave a partially demolished building).
Tethered and Free "Flyers": If the vectored hoist has adequate thrust margins – as well as adequate number, placement, and control of thrusters – then "vectored" sub-systems could potentially serve double duty as elements of "tethered" or even "free" flyer assets whereby these aerial robots could be deployed/support by rotary-wing platforms.
1. To provide access to disaster target sites partially covered with overhanging debris, structures, or natural outcroppings.
2. To provide "low and slow" disaster site aerial coverage, augmenting that of a primary helicopter, via air-deployed (and perhaps air-recovered) vertical lift "free flyers."

The following discussion presents a general outline of a concept of operations (CONOPS) for rescues enabled by the vectored teleoperated rescue hoist. Various operational alternatives are also suggested, wherever appropriate, in this notional CONOPS. This CONOPS will be employed to define notional functional requirements – and operating conditions and parameters of interest – for the conceptual design trade study to follow. The high-rise building rescue CONOPS follows:

1. **Survey.** In addition to their rescue capabilities, helicopters have an essential role to play in performing aerial surveys of disaster/emergency sites. A critical function of such aerial surveys, in connection with rescue lift operations, is identifying acceptable target sites for rescue. For cases where such sites maybe windows or other exterior access points, this problem of identifying acceptable sites will be greatly compounded.

2. **Approach.** Helicopter approaches target recovery point (e.g. an open window or ledge) while maintaining safe/acceptable lateral offset from the building as conditions and aircraft handling permits.

3. **Communicate Intent.** Communication devices, human-system interfaces, and other remote means of conveying intent to those needing rescue should be developed. Ideally, such devices and interfaces would allow for "self-rescue" of victims. Ultimately, though, it is anticipated that, similar to current practices, a member of the aircrew/rescue team will have to be deployed via the vectored hoist to the rescue target site. Unfortunately, though this places the crew/team member in harm's way, it is the only means by which, with high certainty, that safe and effective rescue operations can be performed.

4. **"Reach-Out."** Rescue hoist is deployed to nominal cable length. Helicopter is piloted to relative altitude with respect to target site whereby the hoist free-end, when laterally (and to a lesser extent vertically) is "propelled" by thrusters to the target location. The "vectored" thrusters are operated in one of two ways: (a) under continuous static thrust with a constant ramp rate for the thrusters, or (b) undergoing a periodic "pumping action" employment of the thrusters to achieve limit-cycle pendulum oscillations that closes with the target site location (nearly at) during the "dwell" of the hoist oscillation. This approach to

reaching the target would further entail some form of grapple to be of utility for rescue efforts. (Securing the hoist at the target site will be a critical design problem to address.)

5. **On-Site Presence and Situational Control.** The rescue team member, having been lifted by the vectored hoist to the target rescue site, would secure the hoist and take control of the immediate situation. Upon establishing situational control, rescue operations would commence.

6. **Recovery.** One of several methods could potentially be employed to recover rescue victims (from the target site to safely inside the helicopter cabin). They are: (a) motorized rappelling; (b) "free-swing," (c) "braking action," (d) continuous reduction of static thrust.

7. **Re-Staging/Re-Deployment.** Subsequent redeployments of the vectored hoist would be undertaken (including recovery of the rescue team member) until aircraft capacity is reached.

8. **Clear and Away.** Identify or demark the target site such that the site can be returned to, on need, or "cleared" from further rescue activity.

Figure 3 illustrates the challenges in performing rescues from windows or exterior walls of high-rise buildings using helicopters. Except for rooftop rescues, or from windows/ledges on the very uppermost stories of the buildings, helicopters cannot perform rescues from building exterior walls. This is because rescues from helicopters can only currently be performed for near-vertical lifts.

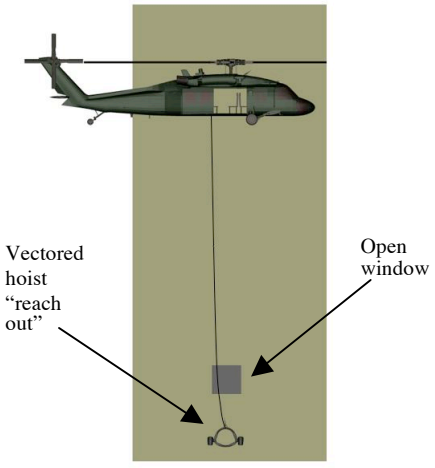

Fig. 3 -- Access through Improvised Exits

Notional Design Requirements & Design Space

The following notional functional systems requirements can be defined on the basis of the high-rise building rescue CONOPS. These initial functional requirements are noted in Table 4.

Table 4 – Functional Requirements

Onboard Operator Control Station
1. Onboard control station controls thrusters at hoist free-end. 2. Provides visual situational awareness and operational status.
Power and/or Fuel System(s)
1. Two options: power and/or fuel system being integrated into free-end of hoist rig or onboard aircraft with plumbing/routing 2. Initial assumption is that power and/or fuel-system is integral to the "free-end" of the hoist rig.
(Optional) Emergency Supply or Device Deployment Mechanism
(Optional) Rappelling Mechanism and Rigging
Communication, Guide-lights, and Instructional Display(s)
Adequate means for communicating between the aircraft and victims, and deployed crew, at the target rescue site needs to be provided for. This potentially includes intercoms and displays mounted on the free-end of the hoist as well as speakers and large-scale aircraft -mounted LED alphanumeric visual displays.
Passenger Harness or Conveyance for Transport and Recovery
Basket versus sling (or other harness type); probably an issue as regards simplicity, ease of use, and speed of access and egress versus security or safety of conveyance
Attach Point Securing Mechanism
Must have a means of securing the hoist rig when thrusters are disabled and the rig is fully extended (i.e. there is considerable side-force "pull," "dithering" motion, and potential energy) to ensure that people are not put in jeopardy while being attached to and recovered by the hoist rig.
Thrusters
1. Physical safeguards to protect people in close proximity to device/hoist when in operation; i.e. screens/vanes for inlet/exit for ducted-fans, or cold- versus hot-gas exhaust from reaction-jets, etc. 2. Capable of being "vectored" i.e. make angular deflection adjustments of either the thruster itself or the thruster vector. 3. Sustained thrust for maximum lateral displacement ($x_{lat} = 2R$) for ten minutes for crew emplacement/recovery; sustained thrust for five minutes per rescue for five rescues.
Snubber
Provides low load "fixed" pivot for cable for hoist apparatus onboard helicopter
"Final Safeguard" Cable Cutter
Cable cutter at fixed-end of hoist to clear cable, in case of fouling, to protect safety of aircraft and aircrew.

These functional requirements will subsequently be considered in a conceptual design trade study. One last important functional requirement to consider in a design study is the minimization of any significant modifications to existing aircraft and, further, to retain/incorporate as much existing rescue hoist design heritage as possible in the vectored rescue hoist conceptual designs.

An example of one major design tradeoff is that between different types of thrusters employed by the vectored rescue hoist. Table 5 summarizes the relative advantages and disadvantages of the two thruster candidates: ducted-fans and cold-gas, or air, jet thrusters.

Table 5 – Thrusters

Advantages	Disadvantages
Ducted-Fan:	
Mature technology with respect to design and analysis methodologies.	Duct inlets/exits have to have protective safeguards (screens or vanes) to avoid ingestion of FOD (foreign object debris) and even extremities of people being transported.
Duct protects people and objects in close proximity to fans; easy to implement protective screening at the duct inlet and exit.	Ducts ideally need to be designed to have debris "positive capture" characteristics for possible fan blade failure.
Cross-cutting technology leveraging with micro VTOL ducted-fan aerial vehicle development efforts	Thruster response to transient control inputs, for compensating for gust or turbulence, is comparatively lower than the alternative.
Cold-Gas, or Air, Jet:	
Simplicity of design and control.	Higher exit velocities as compared to ducted fan
No flammability concerns.	Exhaust exit temperature, due to nozzle expansion, significantly colder than ambient
Mature commercial off the shelf (COTS) solutions for pressure tank hardware.	Significantly less potential thrust output as compared to ducted-fan thruster configurations.
Less potential anxiety of crew and passengers being in close proximity to cold-gas jets than compared to alternative	Potentially severe/hazardous acoustic characteristics requiring exhaust acoustic mufflers.

Figure 4 shows a partial summary of the anticipated design space for vectored rescue hoists. Design solution options for the vectored hoist thrusters, propulsion system, the approach to conveyance of the hoist passengers, and possible means of securing the hoist and transferring passengers to and from the hoist at the target rescue site are noted in the figure.

As can also be seen in Fig. 4, an initial qualitative assessment has been made with respect to elements of this notional design space for the vectored hoist. In particular, this abbreviated assessment has identified a number of key candidate design features have been highlighted for further evaluation. In particular, ducted-fans are the leading candidate for the hoist thrusters. Equally important, it is also noteworthy to recognize that the process of securing the hoist at the target rescue site -- and transferring (on and off the hoist 'free-end") rescue crew and "passengers" -- doesn't reveal a strong candidate for possible implementation in this initial design space assessment. This will remain a critical issue to consider when evaluating various CONOPS approaches for deployment (reaching out) and recovery of team members and recovery of people in need.

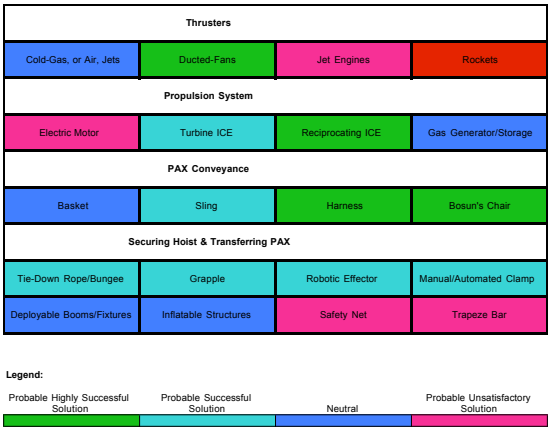

Fig. 4 – Partial Design Space and Initial Qualitative Assessment

Figure 5 illustrates a notional control diagram for the hoist operator (and helicopter pilot) to effect control over a vectored rescue hoist. Alternate approaches (including different sensors and control inputs) could be defined as compared to that shown in Fig. 5, but the essential details of the control challenge are nonetheless presented.

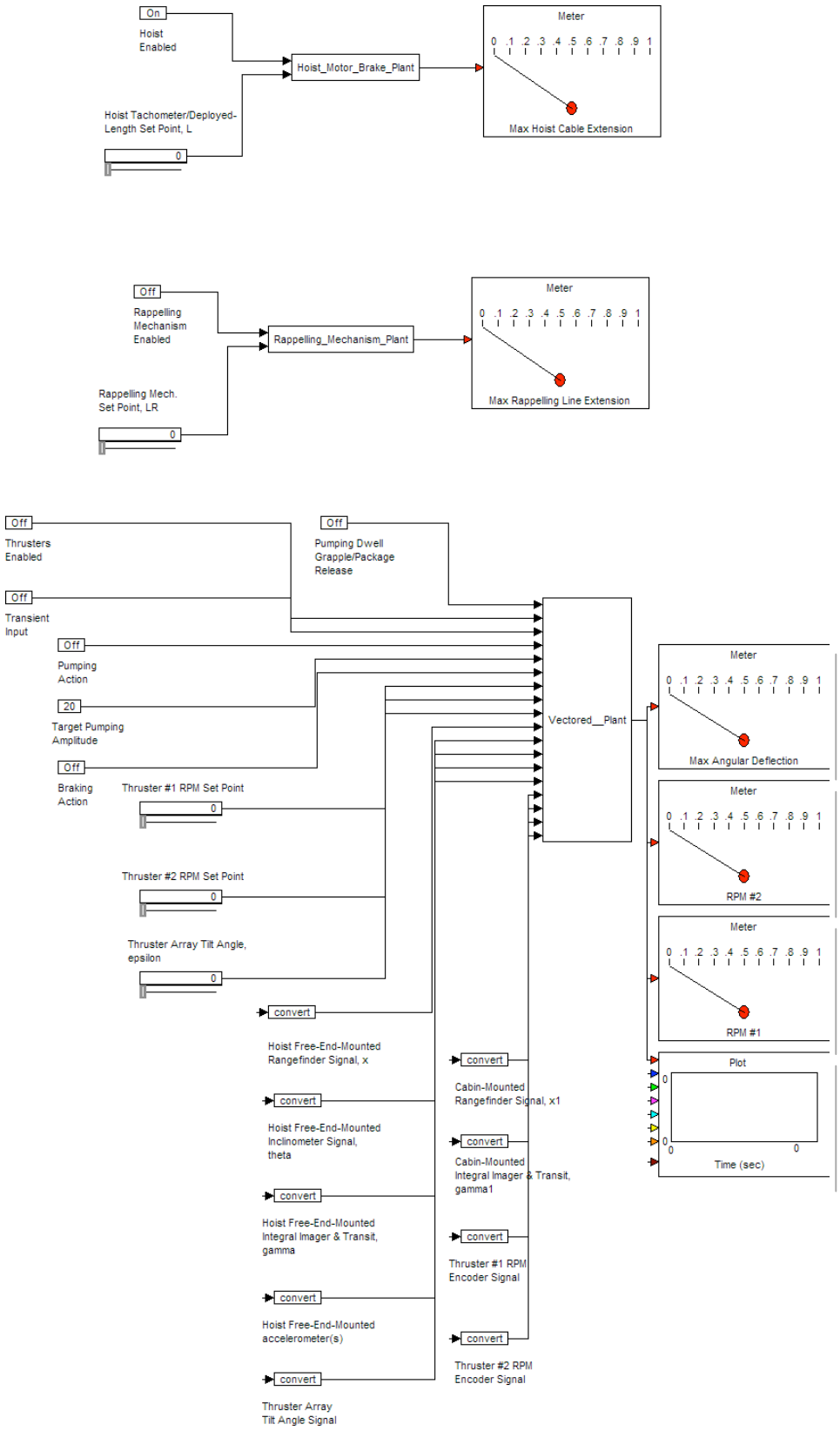

Fig. 5 – Notional Vectored Rescue Hoist Control Diagram

Because of the intrinsic coupling between lateral and vertical displacements of the free-end of the hoist in reaching the target recovery site, an interactive control input process is required (as shown in Fig. 5). This lateral/vertical displacement coupling is best illustrated by noting the following constraint, Eq. 1a-b, that must be preserved during the coordination of the hoist operator and the helicopter pilot. This constraint is derived from geometry considerations.

$$\theta_{target} = 2\delta$$

$$If\left(\left|x - 2\ell \sin^2 \delta\right| > error\right)$$

$$Then\ \ Adjust\ \ \ell\ \ \left(Hoist\ Operator\right)\ \ Or\ \ x\ \ \left(Pilot\right)$$

(1a-b)

Where δ is the relative inclination, from the horizontal plane, from a hoist free-end-mounted imager as measured by a transit, or associated software, of the target recovery site. The parameter θ_{target} is the target angular deflection of the hoist to reach the target point/site with the hoist free-end. The parameter x is the lateral displacement, as measured by a rangefinder sensor, from the un-deflected hoist free-end to the target site vertical plane. Similar relationships and constraints as Eq. 1a-b can be derived for cabin-mounted inclination/transit and rangefinder sensors versus those at the hoist free-end.

In addition to providing for lateral displacement control of the vectored hoist using thrusters, the thruster array (and/or the type of thrusters employed) must also provide for longitudinal (with respect to the aircraft fixed-frame axes) control/displacements. The hoist free-end with be subject to turbulence/gust disturbances that will need to be mitigated with the thrusters. Additionally, the thrusters should ideally act through the center of gravity of the hoist free-end; this will perhaps be difficult to achieve for both cases, with and without payload, being carried by the hoist. Both problems can perhaps be addressed by employing multiple thrusters, adjustable thruster nacelle tilt, and/or thrusters having movable vanes, or, alternatively, thrusters with tandem fans and oval/elliptical ducts.

Preliminary Results

Some first-order assessments of the vectored rescue hoist sizing and operational characteristics will now be presented. The equations and analysis employed in deriving the following results are summarized in the Appendix. For most of the analysis results presented the following parameter values are used: $T_R = 98k\text{N}$; $R = 8.2m$; $V_{Tip} = 213m/s$; $C_T = 0.0085$; $k = 1.15$; $\ell/R = 4$ (unless otherwise noted); $x_o = 0.5R$; $y_o = 0$; $z_o = -0.25R$; $x_{lat} = 2R$; $m_{payload} = 90.7kg$ (200 lbf); $m_{rig} = 45.3kg$ (100 lbf); $\rho_{cable} = 5.2kg/m$; $\varepsilon = \pi/2$; $f_{cable} = 0.0032m^2$ *per unit length, m*; $f_{z_{rig}} = 0.21m^2$; $f_{x_{rig}} = 0.4m^2$; $f_{z_{payload}} = 0.11m^2$; $f_{x_{payload}} = 0.46m^2$. Note that these parameter values are illustrative only and do not reflect an optimal design.

Figure 6a is a superimposed image of a representative rescue helicopter rotor wake in hover, using a simple model detailed in the Appendix, and Fig. 6b presents profiles at various different axial stations of the vertical induced velocities from that same rotor wake model.

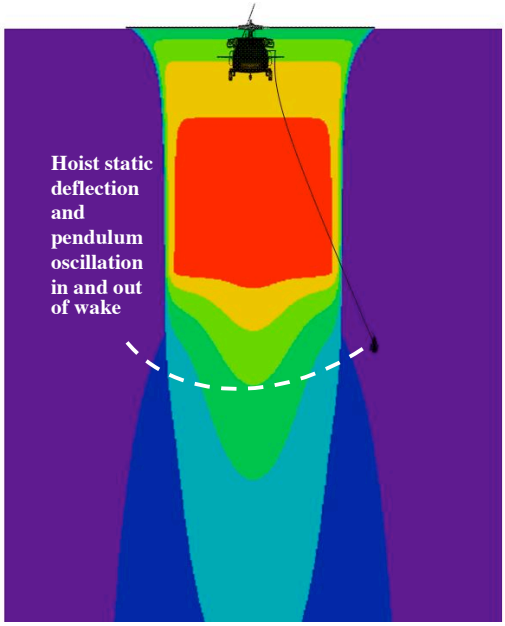

(a)

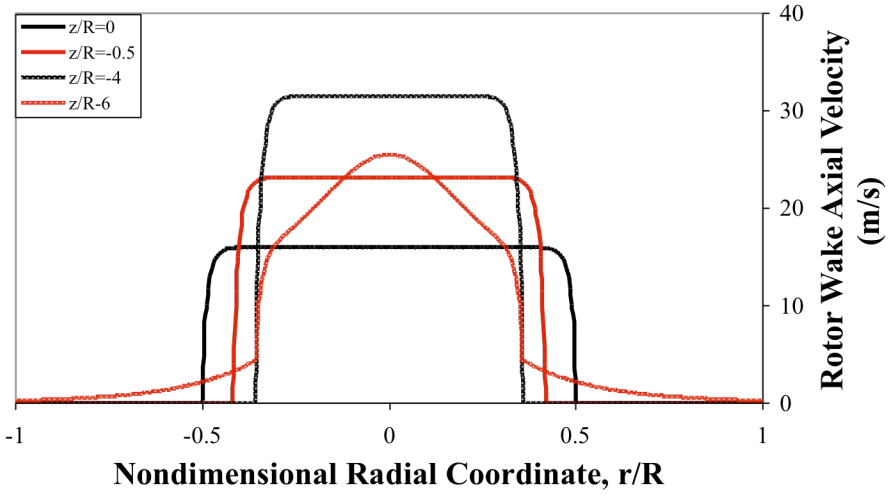

(b)

Fig. 6 – Representative Rotor Wake Model Results: (a) global flow field and (b) induced vertical velocity profiles as a function of axial coordinate

The rotor wake model is only approximate in nature. It is not intended to compete with far more accurate methods for hover flow field predictions. Further, the approximate model does not include airframe wake blockage effects, or wake interactions with large bodies or surfaces such as buildings and or the ground. Nonetheless, it does incorporate the important influence of wake contraction in the near-wake and the transition to jet-like flow in the far-wake. It is more than accurate for the rescue hoist assessments that follow.

Simulation of Static Thrust "Reach-out" (controlled lateral displacement)

Figure 7 illustrates the vectored rescue hoist concept achieving lateral displacement using static thrust from a set of onboard ducted-fan thrusters. The magnitude of the target lateral displacement, x_{lat}, is a key design driver for the vectored rescue hoist. Too small of x_{lat} will lead to obstacle collision and hazard avoidance issues; too large of x_{lat} will result in too large of static thrust levels demanded of the vectored thrusters.

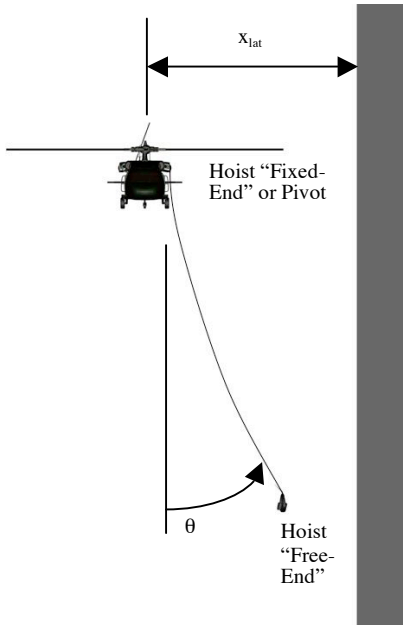

Fig. 7 -- Extending Rescue Hoist Lateral Reach

A Runge-Kutta ordinary differential equation (ODE) solver from a commercial engineering software package was used to solve the differential equations describing the vectored rescue hoist's pendulum-like dynamics. Before discussing the hoist dynamics, though, the static thrust versus deflection characteristics will be presented. Figure 8 illustrates these static deflection characteristics for two different hoist rig weights; these curves were defined by use of a Newton-Raphson algebraic equation solver. There are only slightly

discernable nonlinearities with these pendulum "spring rate" curves. Further, the influence of the hoist/rotor-wake interaction cannot be readily seen because of the relatively small contribution of the hoist aerodynamics to the effective spring rate as compared to the gravity effect.

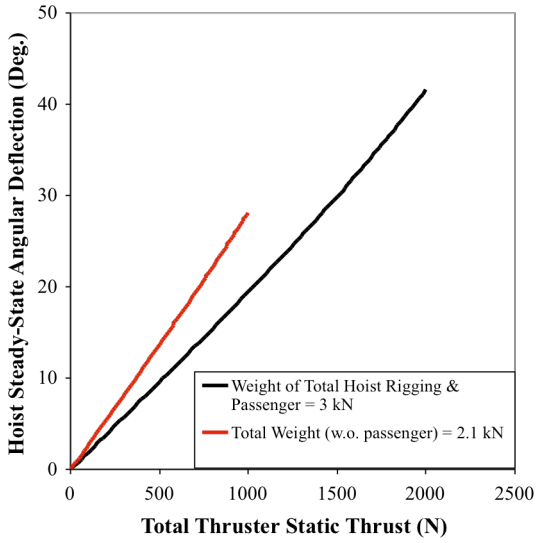

Fig. 8 – Steady-State Hoist Angular Deflection as a Function of Total Thruster Static Thrust

Very low levels of aerodynamic damping for the vectored rescue hoist pose significant control challenges. (No structural damping is assumed in the analysis.) These problems are not insurmountable but will possibly entail some level of control stability augmentation in order to avoid unacceptable station-keeping oscillations. Figure 9, by way of example, shows two thruster ramp rates studied as to their influence on hoist dynamics for hoist "reach out," or rather, deployment.

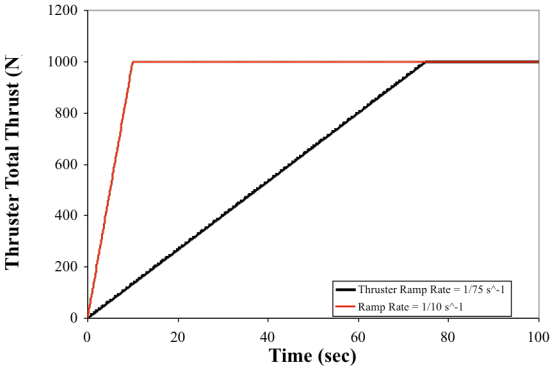

Fig. 9 – Examples of Thruster Ramp Rates

Figures 10a and 11a illustrate the influence of thruster ramp rate (inverse of the time required to apply full thruster load to achieve the steady-state target angular deflection) on the magnitude of target "station-keeping" oscillation due to low aerodynamic damping. Not unexpectedly, low thruster ramp rates result in low (cycle limit type) oscillations about the nominal target angular deflection and quasi-steady shear forces. Figures 10b and 11b show the corresponding time trends of the hoist "fixed-end" pivot shear forces.

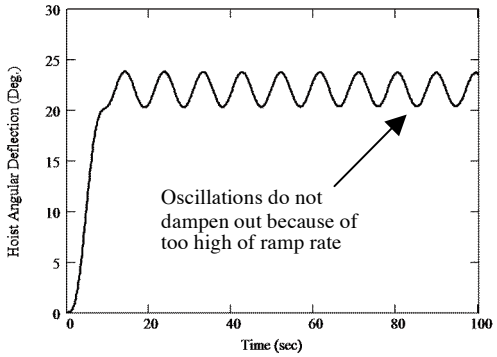

(a)

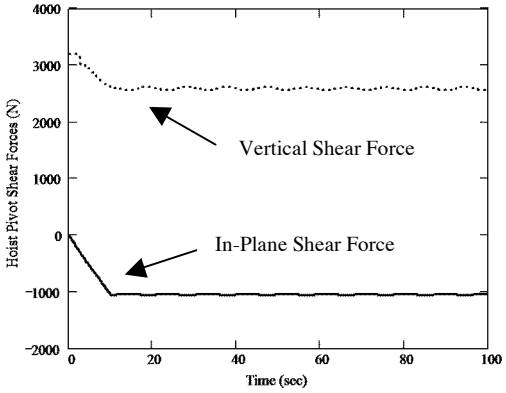

(b)

Fig. 10 – Thruster Ramp Rate (zero to full throttle) of 1/10 s^{-1}: (a) Hoist Angular Deflection as a function of time and (b) Pivot Shear Forces

Point of fact, it can readily be seen that reasonably low ramp rates can be imposed that result in well-behaved oscillatory station-keeping characteristics. However, it is important to note that the effect of gusts, rotor wake unsteadiness, and helicopter transient motion has not been accounted for in this analysis and will, therefore, pose additional challenges for maintaining stable station-keeping for the vectored rescue hoist "free-end."

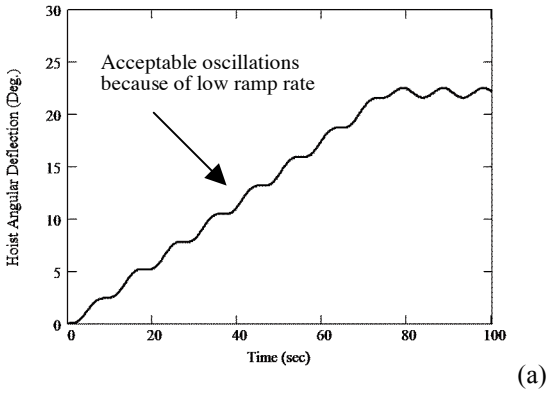

(a)

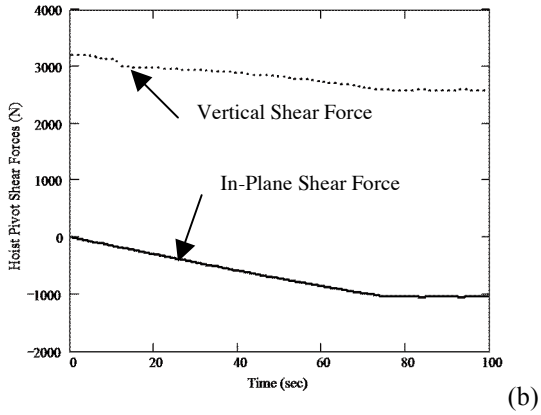

(b)

Fig. 11 – Thruster Ramp Rate (zero to full throttle) of 1/75 s^{-1}: (a) Hoist Angular Deflection as a function of time and (b) Pivot Shear Forces

Simulation of "Free-Swing" Recovery

One possible recovery option is to employ a "free-swing" strategy. This basically entails safely harnessing the rescue victim in the "vectored" hoist apparatus, releasing the hoist safety tie-down, and letting the hoist and passenger swing out and away until pendulum-like the hoist settles directly below the helicopter and a conventional vertical lift can be executed (Fig. 12).

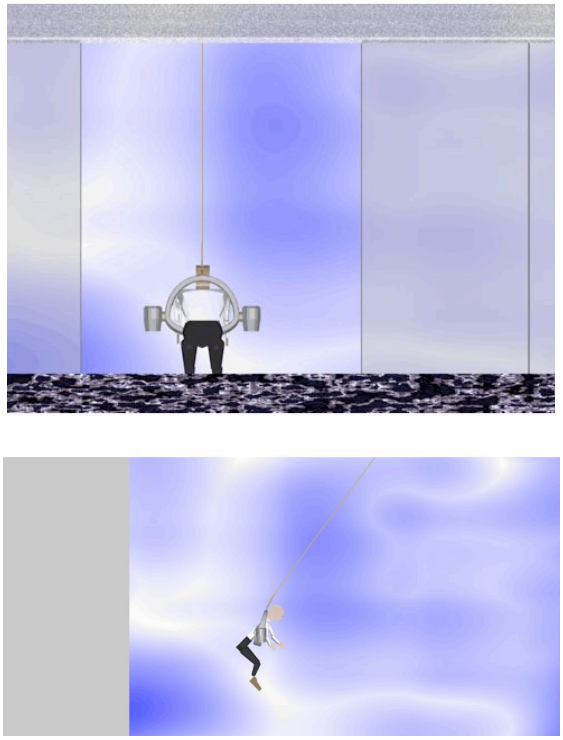

Fig. 12 – Free-Swing Recovery

The "free-swing" approach makes for a simple and efficient (albeit anxiety-inducing) recovery. The key problem with the "free-swing" recovery approach is that the aerodynamic damping of the rescue hoist is so comparatively low with respect to the hoist dynamics that the hoist angular oscillations take a great deal of time to decay. The slow "free-swing" oscillation decay can be clearly seen in Fig. 13.

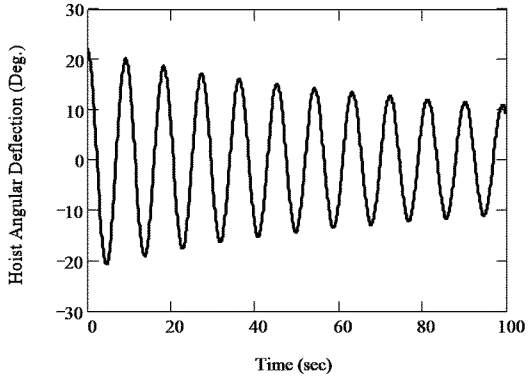

Fig. 13 – "Free-Swing" Recovery (Angular Deflection versus Time)

The influence of the hoist aerodynamics and interaction with the rotor wake can be seen in Fig. 14. The hoist/rotor-wake interactions are asymmetric with respect to the hoist angular deflection, θ, because of the large lateral offset defined for the hoist fixed-end pivot location, x_O.

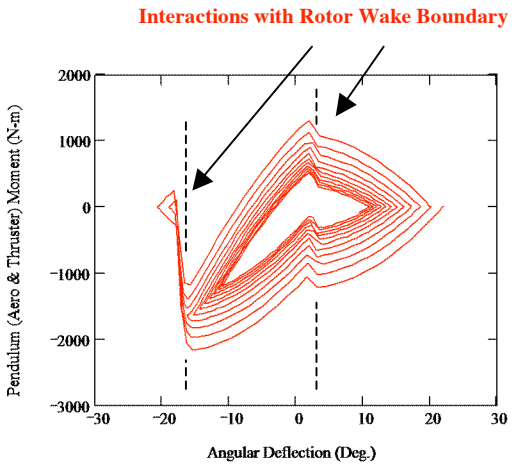

Fig. 14 – Hoist Aerodynamic Moment as a Function of Angular Deflection (Multiple Cycles of Oscillation) During "Free-Swing" Recovery

The corresponding "free-swing" vertical and in-plane "fixed-end," or pivot, shear forces can be seen in Fig. 15. As can be seen the vertical shear force is both larger in terms of absolute magnitude as well as the oscillatory contributions, as compared to the in-plane shear force.

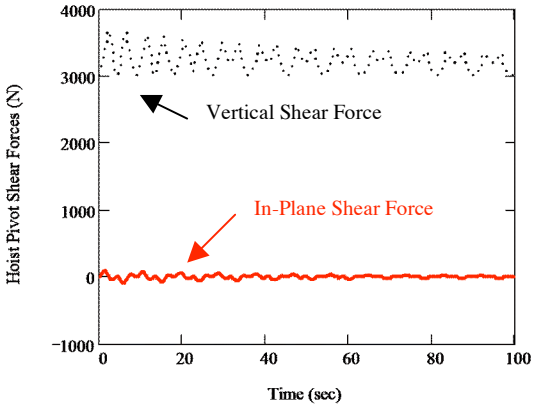

Fig. 15 – Pivot Shear Forces During "Free-Swing"

Given the wild gyrations that a hoist passenger would have to likely undergo in order to execute a "free-swing" recovery, it is hard to imagine that this recovery approach would be adopted for all but the direst of circumstances. Better approaches need to be employed.

Simulation of Thruster "Braking Action" Recovery

As it does not appear, as matter of routine recourse, that the "free-swing" recovery approach is practical, it is necessary to study alternate approaches to recovery problem. One possible alternative is the use of thruster "braking action" during the recovery to actively dampen out the hoist pendulum oscillations. Figure 16 is an illustration of the resulting effective damping during recovery using the thruster "braking action" approach. Comparing the "free swing" oscillations, noted in Fig. 13, with that of the thruster "braking action" oscillations, it is clear that the later approach would provide a substantially better "ride" experience for passengers being recovered.

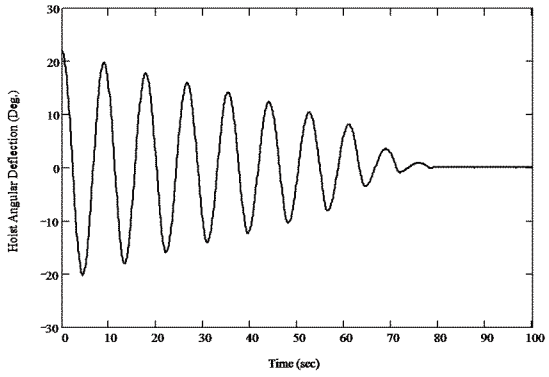

Fig. 16 – Hoist Oscillations during Recovery Using the "Braking Action" Approach

The thruster "braking action" is implemented in the simulation by means of the following "pulsed" type of thruster control, whereby

$$T = if\left(\theta \le 0, if\left(\dot{\theta}_{Lim} \le \dot{\theta} \le 0, 1, 0\right), 0\right) \cdot \sum_i T_i \qquad (2)$$

Where the lower angular velocity limit, $\dot{\theta}_{Lim}$, is subject to the constraints $\dot{\theta}_{Lim} < 0$ and $\left|\dot{\theta}_{Lim}\right| << \max\left(\dot{\theta}\right)$; specifically, for the simulation results presented in Fig. 16, $\dot{\theta}_{Lim} \approx -0.1\ rad/s$.

This periodic "pulsed" braking application of the thrusters (physically realizable with cold-gas, or air, jet thrusters, but only approximately so for ducted-fan thrusters) is perhaps best illustrated by considering the hoist pivot shear forces, Fig. 17. The "pulsed" application of the thrusters can be seen in the in-plane shear force time history.

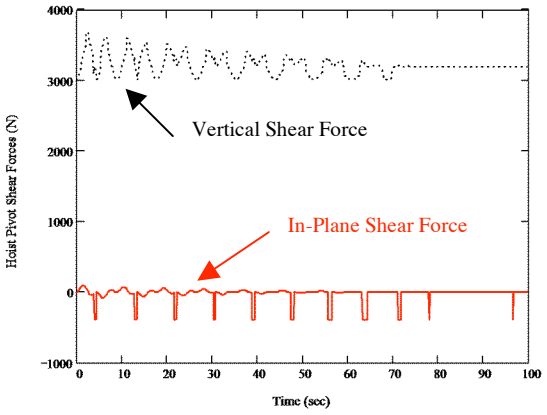

Fig. 17 – Pivot Shear Force Time Trends During Thruster "Braking Action"

Only a fraction (~40% in Fig. 16) of the static thrust required for the original vectored rescue hoist (steady-state) "reach out" to the initial angular deflection condition was required to effect the "braking action." In this regards the "braking action" approach is more efficient in terms of thruster energy expended than effecting a quasi-steady ramp-down of the thruster to effect recovery.

"Rappelling" Recovery

An alternate (to the "free-swing" and "braking action") recovery approach would be to employ motorized rappelling of the hoist. This rappelling approach has a couple of advantages over the "free-swing." First, it is more perhaps consistent with current procedures using "guidelines" to expedite ground recovery of victims. Second, it may be perceived as more controlled and, therefore, perhaps safer. The biggest disadvantage of the motorized rappelling approach is the relatively slow pace of recovery as compared to the "free-swing" or thruster "braking action" approaches. Additionally, a great deal of cabling weight (both for the hoist and the rappelling mechanism) must be suspended from the helicopter. This additional weight increases the static thrust required to "reach out" to the target site initially and, therefore, increases the size of the thrusters required.

Interestingly enough the vectored hoist configuration wherein people can be rescued by motorized rappelling to/under the helicopter and then retraction by the main hoist winch/motor is analogous to similar kinematic problems studied in Ref. 11, for cable-suspended robots. Figure 18 illustrates the rappelling option for the recovery of people.

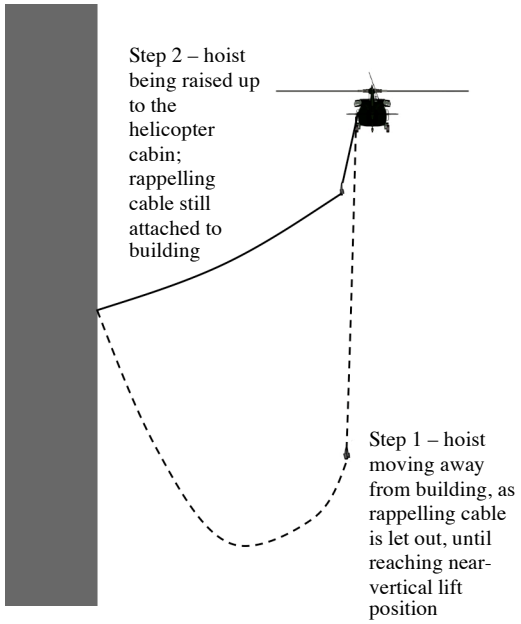

Fig. 18 -- Notional Rappelling Recovery Option

From an energy expenditure perspective, the rappelling recovery approach is perhaps the optimal recovery solution. Not only is the energy expended to return the hoist to near-vertical-lift position less than that achievable by static thrust or by braking action, but the rappelling mechanism can be left attached upon recovery of the first rescue victim such that subsequent recoveries (for a single helicopter flight) can be solely effected by hoist and rappelling mechanism cable extension and retraction and not by thruster application.

Simulation of "Pumping" Action "Reach-out"

There may be circumstances whereby the static thrust provided by the vectored rescue hoist is insufficient to carry the required payload weight to the target steady-state target hoist angular deflection. For these special cases, it may be necessary to, in transient manner, achieve the maximum angular deflection at the "dwell" of the hoist pendulum upswing. This thruster "pumping action" is similar to but subtly different from the "braking action" discussed earlier. In both cases, though, "pulsed" control of the hoist thruster is required. The conditional control logic used to implement the "pumping action" is as follows

$$T = if\left(\theta \geq 0, if\left(0 \leq \dot{\theta} \leq \dot{\theta}_{Lim}, 1, 0\right), 0\right) \cdot \sum_i T_i \tag{3}$$

Where the upper angular velocity limit, $\dot{\theta}_{Lim}$, is subject to the constraints $\dot{\theta}_{Lim} > 0$ and $\left|\dot{\theta}_{Lim}\right| << \max\left(\dot{\theta}\right)$; specifically, for the simulation results presented in Fig. 19, $\dot{\theta}_{Lim} \approx 0.1\ rad/s$.

Figure 19 illustrates the hoist oscillatory deflections subjected to thruster "pumping." For a fraction of the thrust (~20%) required for statically deflecting the hoist to the target angular deflection, the "pumping action" efficiently achieves (in a transient sense) the target angle.

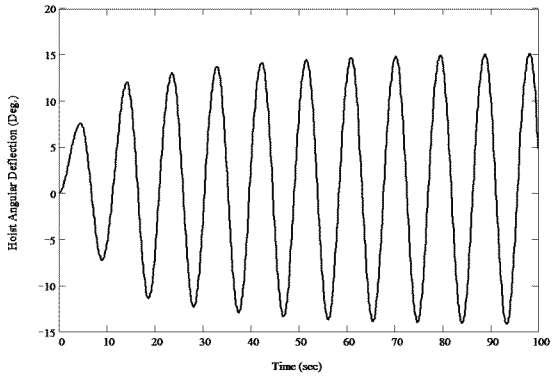

Fig. 19 – Thruster "Pumping Action" for Transient "Reach Out"

The effective action of the "pulsed" thruster for the "pumping action" can be seen in the hoist "fixed-end" pivot shear forces, Fig. 20. In particular, the in-plane shear force time history reveals that both the duration and time phase of the thruster pulses for the "pumping action" changes with time. Consequently, the hoist oscillations reach a limit cycle with respect to maximum angular deflection rather than grow exponentially unbounded.

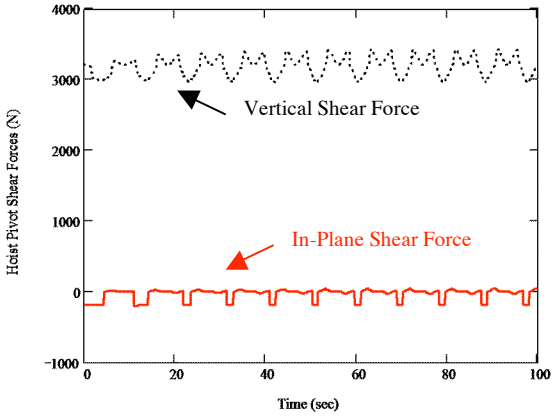

Fig. 20 – Hoist "Fixed-End" Pivot Shear Force Time Trends Subject to Thruster "Pumping Action"

This resulting limit cycle is perhaps better illustrated in Fig. 21. The wedge-shaped envelope is the final resulting hoist deflection cycle limit. The series of vertical lines below the wedge-shaped limit envelope are the successive pulses of the thruster implementing the "pumping action." The horizontal shift in these pulse lines reflect the time phase shift of the thruster "pumping" as determined by the conditional control logic embodied in Eq. 3.

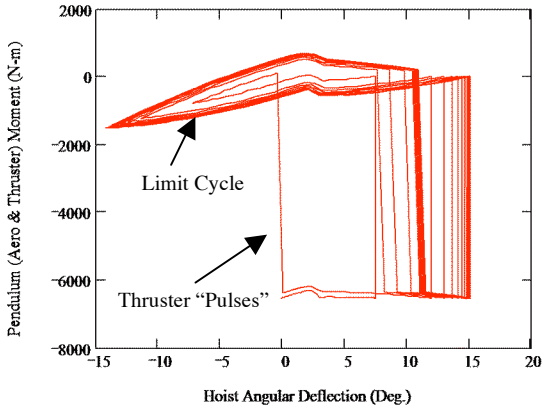

Fig. 21 – Resulting Cycle Limit for Suggested "Pumping Action" Control Logic

Some of the emergency response tasks/applications where such a means of achieving large transient hoist excursions include: release of a grappling hook or other quick-release attachment device at the hoist dwell point to arrest the swinging motion of the hoist at its peak angular deflection; relying on the sling shot effect of the vectored hoist to "catapult" small packages/payloads of critical emergency equipment into otherwise inaccessible locations.

Thruster Sizing

Four sizing cases will now be considered. First, vectored hoist using ducted-fan thrusters for the case that $W_{payload} = 0$ or $W \rightarrow W_{rig} + W_{cable}$. Second, ducted-fan thrusters used for the case that $W_{payload} = 0.9\text{kN}$ or (200 lbf). Third, the vectored hoist employing periodic "pumping action." And, fourth, the vectored hoist thrusters being employed to perform periodic "braking action."

Figure 22a-c show the trends of thruster static thrust required as a function of hoist cable length for various different parametric influences. Among those parameters are the design target for the hoist lateral displacement, x_{lat}, the anticipated hoist rig weight, W_{rig}, and the cable per unit length mass, ρ_{cable}. In all these cases, Fig. 22a-c, there appears to be a point whereby increasing cable length no longer significantly reduces the thrust required from the hoist thrusters to achieve the required lateral displacement, x_{lat}.

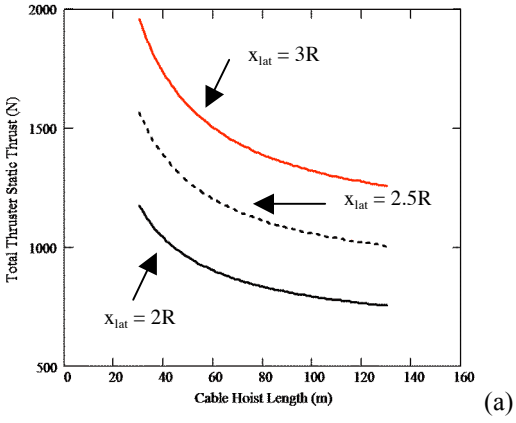

(a)

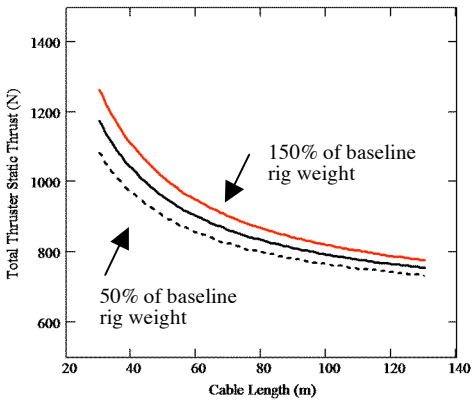

(b)

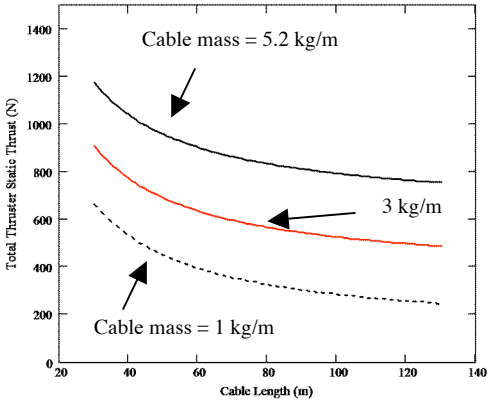

(c)

Fig. 22 – Thrust required as a function of cable length: (a) different lateral displacement targets, (b) different fractions of assumed baseline rig weight, and (c) different cable kg/m

Figure 23 presents ducted-fan thruster sizing trends for two different disk loadings – 960 N/m^2 (or 20 psf) and 1915 N/m^2 (40 psf) -- that are representative of the high loadings typical of ducted-fan thrusters.

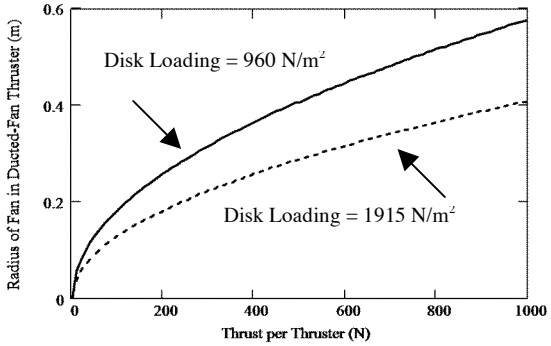

Fig. 23 – Ducted-Fan Thruster Sizing Trends

Figure 24 presents some first-order power estimates for vectored rescue hoists employing ducted-fan thrusters. A simple "rule of thumb" power versus thrust tradeoff is shown in Fig. 24 for a range of disk loadings, $DL \equiv T/A_{DF}$, and anticipated static thrust figures of merit, FM. (As noted in Ref. 12, for example, a static thrust figure of merit of ~0.5 at DL=1490 N/m^2 (or 31 psf) for ducted-fan of the same general size category as anticipated for a vectored thruster (R_{DF}=0.48m) is not unreasonable, given small-scale experimental results reported in that paper.) Given the power levels required for a single thruster it is likely that electric propulsion would not be feasible for this application and that, therefore, a turbine or reciprocating internal combustion engine would be required as the primary power plant. In turn, this would likely dictate a fuel supply integrated into the "free-end" module of the vectored hoist. More refined analyses can be based, in part, on the sizing equations provided in the Appendix.

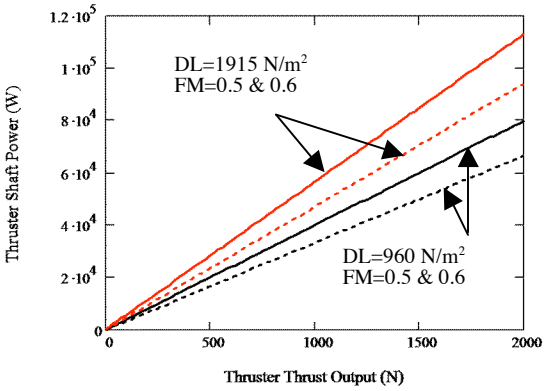

Fig. 24 – Simple Ducted-Fan Thruster Thrust versus Power Trade

If it were not for the penalty of having to support the cable and payload weights, from a thrust and power perspective the thrusters employed for the vectored hoist concept could easy act as propulsion for small autonomous "free flyer" aerial vehicles. This merely reinforces the expectation that the development of vectored rescue hoist systems will by necessity proceed hand in hand with the development of small ducted-fan VTOL UAVs.

Given the simple trade exercise embodied in Figs. 23 and 24, and the earlier hoist pendulum simulation results, Table 6 provides a simple illustration of how different operations with a vectored rescue hoist (responding to different CONOPS scenarios) could influence thruster design characteristics. (Two thrusters are assumed; thruster characteristics are for a single thruster; $\ell/R = 4$; $x_{lat} = 2R$.) As can be seen, the lower the thrust demand for the vectored hoist the smaller the size and significantly lower the power required for the thruster. Correspondingly, the smaller the thrusters required the more likely the overall feasibility of such a system being developed and fielded.

Table 6 – General Influence of CONOPS Approaches on Thruster Characteristics

Thruster Usage	T (N)	R_{DF} (m)	P_{DF} (kW)
Static thrust "reach-out" or recovery (without payload)	398	~0.26-0.36	~13.2-22.5
Static thrust "reach-out" or recovery (with 890N, or 200 lbf, payload)	564	~0.31-0.43	~18.7-31.81
Pumping action "reach out" (Fig. 19)	100	~0.13-0.18	~3.3-5.6
Braking action recovery (Fig. 18)	200	~0.18-0.26	~6.6-11.3

If static thrust deployments and recoveries of a vectored hoist can be avoided, then the hoist's thrusters can be made significantly smaller and lower in power. Or, if the static thrust deployment of a rescue team member can be avoided (instead, perhaps, relying upon remote communication of intent to rescue victims or, alternatively, rappelling of the crew member into position at the target site upon initial unattended securing of the hoist), then the thruster size could potentially be greatly reduced. Significantly more detailed examination of operational issues with the end-user community would be necessary to determine if such CONOPS trades are indeed viable. The above simple sizing trade exercise merely illustrates the challenges of designing a vectored rescue hoist from a thruster aero-performance perspective.

Future Work – Improvements in Analysis

Very simple models for the rotor wakes and "slung load" dynamics were employed in this paper. More comprehensive and complex models – accounting for example the helicopter flight dynamics and the urban canyon operational environment -- will be required to fully establish the feasibility of the vectored rescue hoist concept.

One key issue for consideration in future design and dynamics analysis is the influence of cable dynamics on the vectored rescue hoist. Cable inertial loads, propagating as waves along the cable length due to coupling effects with the vehicle dynamics, could have a profound effect on not only hoist "free-end" station-keeping/positioning but on structural integrity of the hoist, and the safety of people in close proximity to, or being carried/recovered by, the hoist. Another set of potential issues related to hoist control and overall station-keeping is, first of all, the turbulence and gusts of the urban canyon environment as well as, second, the unsteady flow components of the rotor wake. Another important issue is fully three-dimensional dynamics modeling of the vectored host concept, including any torque coupling effects of the thrusters on the hoist dynamics. Finally, it is important to continue to be cognizant of the potential for instabilities for helicopter slung loads and the corresponding implications of such instabilities on the successful implementation of a vectored rescue hoist. Significantly more refined modeling and analysis will be necessary to examine this and similar issues.

Additional Robotic/Augmented Capabilities

The question might be asked: in what context can the vectored rescue hoist concept be considered a *robotic* rescue device? The answer, though perhaps subtle, is that: (1) the vectored hoist is teleoperated, (2) might likely require some sort of stability augmentation system, (3) might require advanced two-way visual and voice communication, (4) might require simple human-system interfaces for both on-the-fly hoist-training/usage for assisted-help by victims, (5) interface/coordinate with other onboard-rescue-helicopter devices/systems for communication, treatment/support pre-staging (such as remote diagnosis and triage assessments), and other mission task execution.

The general mission scenario (rescue from high-rise buildings) implied in the above analysis is not the only mission that might gain considerable utility from the vectored rescue hoist concept. Nor is this mission the only one that might gain advantage from robotic rescue devices deployed from rotary-wing aerial platforms. Table 3, presented at the beginning of the paper, summarized a number of alternate missions that vectored rescue hoist or robotic derivatives might be able to perform. Among the various robotic enhancements that might be applied to the vectored hoist are, for example, robotic arms/effectors to remotely position, attach, and anchor (as need be) the vectored hoist to the rescue pick-up site. Another robotic enhancement might entail the transport and release from the hoist of mobile robotic platforms to perform surveys on the ground or within structures. There are many other possibilities for robotic rescue devices derived from or supported by the vectored rescue concept.

Concluding Remarks

The helicopter has had a critical role in emergency response and disaster relief since its first practical inception. A key component of the helicopter's innate capability for emergency and disaster relief missions is its ability to perform vertical rescue lifts.

The utility of helicopters for emergency response and disaster relief can be greatly enhanced by incorporating and employing advanced teleoperated and/or robotic systems for rescue lift capability. One such concept is explored in this paper – the "vectored" rescue hoist. A notional concept of operations was defined for high-rise building rescues. A number of design issues and possible solutions were detailed. Finally, simple analyses were performed with respect to the vectored rescue hoist concept, given the CONOPS deployment/recovery options identified. The analysis reinforced the life-saving potential for vectored hoist concept but many issues yet remain to be studied. Chief among these issues needing further study is improved dynamic modeling and simulation beyond that using the simple pendulum model used in this paper. The practical utility of such a system may be contingent upon the usage of "transient" vectored hoist pumping and/or braking action inputs (which minimizes thruster size/power) rather than "static" thrust inputs (which require

much larger ducted-fan thrusters). Finally, safely and effectively securing the vectored hoist at the target recovery site for transport of rescue team members and people requiring aid/rescue will be a critical design and operational issue.

References

1. http://www.sikorskyarchives.com/first.html

2. Young, L.A., "Future Roles for Autonomous Vertical Lift in Disaster Relief and Emergency Response," Heli-Japan 2006: AHS International Meeting on Advanced Rotorcraft Technology and Life Saving Activities, Nagoya, Japan, November 15-17, 2006.

3. U.S. Patent # 5020742, "Airborne Rescue System," Inventor: Haslim, L., Publication Date: June 4, 1991.

4. U.S. Patent #5375795, "Fixed Rescue Basket for Helicopters," Inventor: Strunk, H., Publication Date: December 27, 1994.

5. Georgia Institute of Technology "VTOL Urban Rescue Vehicle" 2003 AHS Student Design Competition Entry: http://www.asdl.gatech.edu/design_competitions/

6. U.S. Patent #4588148, "Helicopter Rescue Device," Inventor: Krauchick, W., Publication Date: May 13, 1986.

7. U.S. Patent #3934847, "Rescue Capsule for Use with a Helicopter," Inventor: Bentivegna, P.P., Publication Date: January 27, 1976.

8. U.S. Patent #3931868, "Emergency Rescue Device," Inventor: Smith, Jr., C.P., Publication Date: January 13, 1976.

9. Nishi, A. "A Wall Climbing Robot Using Propulsive Force of Propeller," Fifth International Conference on Advanced Robotics: 'Robots in Unstructured Environments', Pisa, Italy, June 19-22, 1991.

10. University of Maryland "VTOL Urban Rescue Vehicle" 2003 AHS Student Design Competition Entry: http://www.enae.umd.edu/AHS/design/

11. Roberts, R.G., Graham, T., and Lippitt, T., "On the Inverse Kinematics, Statics, and Fault Tolerance of Cable-Suspended Robots," Journal of Robotic Systems, Vol. 15, No. 10, 1998, pp. 581-597.

12. Abrego, A.I. and Bulaga, R.W., "Performance Study of a Ducted Fan System," AHS, International, Specialists Meeting on Aerodynamics, Acoustics, and Test and Evaluation, San Francisco, CA, January 23-25, 2002.

13. Vierck, R.K., *Vibration Analysis, 2nd Ed.*, Harper & Row, Publishers, New York, NY, 1979.

14. Hoerner, S.F., *Fluid-Dynamic Drag*, Self-published, 1965.

15. Young, L.A., Aiken, E.W., Derby, M.R., Johnson, J.L., Navarrete, J., and Demblewski, R., "Engineering Studies into Vertical Lift Planetary Aerial Vehicles," AHS International Meeting on Advanced Rotorcraft Technology and Life Saving Activities, Utsunomiya, Tochigi, Japan, November 11-13, 2002.

16. Cahn, M.S., "The Design and Performance of Shrouded Propellers," National Aerospace Engineering and Manufacturing Meeting, Society of Automotive Engineers, Paper 587C, Los Angles, CA, October 8-12, 1962.

17. Stepniewski, W.Z. and Keys, C.N., *Rotary-Wing Aerodynamics*, Dover Publications, Mineola, NY, 1984.

18. Johnson, W., *Helicopter Theory*, Princeton University Press, Princeton, NJ, 1980.

19. Wake, B.E., Owen, S.J., and Egolf, T.A., "Navier-Stokes and Euler Solutions for an Unmanned Aerial Vehicle," AIAA CP 92-2609, AIAA 10th Applied Aerodynamics Conference, Palo Alto, CA, June 22-24, 1992.

20. Guerrero, I., et al, "A Powered Lift Aerodynamic Analysis for the Design of Ducted Fan UAVs," AIAA 2003-6567, 2nd AIAA "Unmanned Unlimited" Meeting, San Diego, CA, September 15-16, 2003.

21. Fleming, J., et al, "Improving Control System Effectiveness for Ducted Fan VTOL UAVs Operating in Crosswinds," AIAA 2003-6514, 2nd AIAA "Unmanned Unlimited" Meeting, San Diego, CA, September 15-16, 2003.

22. Fusato, D., Guglieri, G., and Celi, R., "Flight Dynamics of an Articulated Rotor Helicopter with an External Slung Load," Journal of the American Helicopter Society, Vol. 39, No. 4, 2002.

23. Cicolani, L.S., and Kanning, G., "Equations of Motion of Slung-Load Systems, Including Multi-lift Systems," NASA TP 3280, November 1992.

24. Bisgaard, M., Bendtsen, J.D., and la Cour-Harbo, A., "Modeling of Generic Slung Load System," AIAA Modeling and Simulation Technologies Conference, Keystone, CO, August 21-24, 2006.

25. Stuckey, R.A., "Mathematical Modeling of Helicopter Slung-Load Systems," Australian Defense Science and Technology Organization (DSTO), DSTO-TR-1257, December 2001.

26. Young, L.A. and Derby, M.R., "Rotor/Wing Interactions in Hover," NASA TM 2002-211392, April 2002.

27. Gauntner, J.W., et al, "Survey of Literature on Flow Characteristics of a Single Turbulent Jet Impinging on a Flat Plate," NASA TN D-5652, February 1970.

28. Pai, S.I. *Fluid Dynamics of Jets*, D. Van Nostrand, Company, New York, NY, 1954.

29. White, F.M., *Viscous Fluid Flow*, McGraw-Hill, 1974.

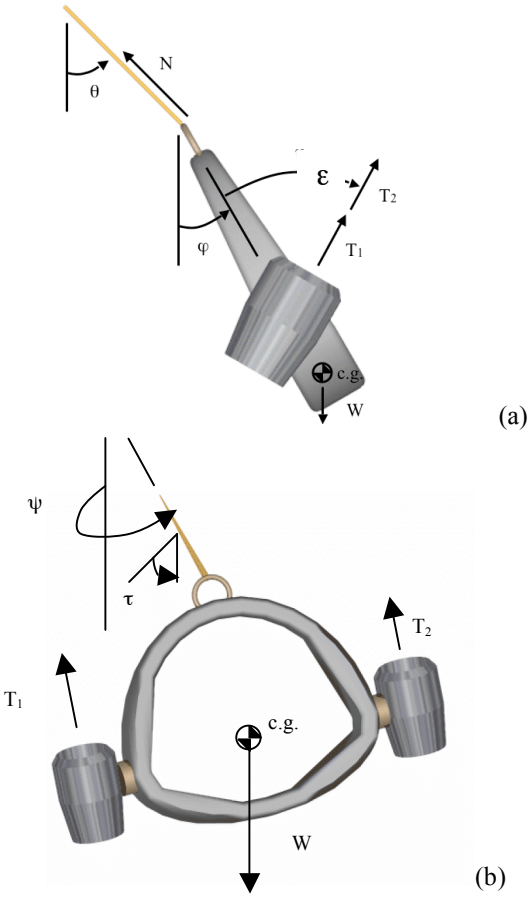

Fig. 25 -- Relative Angular Displacements of Vectored Hoist: (a) x-z plane and (b) y-z plane

Appendix – Analysis

The following discussion in this Appendix summarizes the key equations and analysis used in this paper. Key to this overall analysis is the development of a simple pendulum dynamics model for a vectored hoist employing ducted-fan thrusters. In addition to the pendulum dynamics models additional analysis models are summarized for the rotor wake in hover as well as analysis related to ducted-fan thrusters. The rotor wake model though simple and only approximate in nature does model both the near-field wake which is based on classic actuator disk and vortex theory and the far-field wake which takes on jet-like flow behavior.

Pendulum/Slung-Load with External Forcing

The majority of the analysis performed is completed assuming a simple pendulum model of the vectored rescue hoist. Making the assumption that the hoist rig can be represented as a point mass, the motion is restricted to a two-dimensional plane, that $\varphi \approx \theta$, and pivot location is fixed in space. The applicable equation of motion is the classic pendulum equation (see e.g. Ref. 13) with an added moment term, M, included (Eq. 4a-g). The moment term, , accounts for the aggregate influence of multiple thrusters, the influence of both horizontal and vertical drag of the hoist components on both aerodynamic effective damping and spring rates of the pendulum motion.

$$I\ddot{\theta} + W\ell\sin\theta + M = 0$$

Where

$$I \approx \frac{\ell^2}{g}\left(W_{rig} + W_{payload} + \frac{1}{3}W_{cable}\right)$$

$$W = W_{rig} + W_{cable} + W_{payload}$$

$$M = M_E + M_W + M_T$$

$$M_E = 0$$

$$M_T = -\ell\sin\varepsilon \cdot \sum T_i$$

$$M_W \approx \frac{1}{2}\left\{\left(f_{z_{rig}} + f_{z_{payload}}\right)v_z^2 + \frac{1}{2}\chi f_{cable}\, v_{ze}^2 \cdot \sin^3|\theta|\right\}\rho\ell\sin\theta + \frac{1}{2}\left(f_{x_{rig}} + f_{x_{payload}} + \frac{1}{8}f_{cable}\right)\rho\ell^3 signum(\dot{\theta})(\dot{\theta})^2$$

(4a-g)

In the above, the rig, payload, and cable flat plate vertical drag area parameters are respectively given by: $f_{z_{rig}} \equiv C_{Dz_{rig}} S_{z_{rig}}$, $f_{x_{rig}} \equiv C_{Dx_{rig}} S_{x_{rig}}$, $f_{z_{payload}} \equiv C_{Dz_{payload}} S_{z_{payload}}$, $f_{x_{payload}} \equiv C_{Dx_{payload}} S_{x_{payload}}$, $f_{z_{cable}} \equiv C_{Dz_{cable}} S_{z_{cable}}$, $f_{x_{cable}} \equiv C_{Dx_{cable}} S_{x_{cable}}$, and $f_{cable} \equiv C_{d_{cable}} S_{cable}$. The cable flat plate vertical drag area parameter, f_{cable}, is defined for flow normal to the cable cross-section; cable drag for yawed flow is accounted for in the $\sin^3\theta$ term (see the cylinder cross-flow discussion in Ref. 14). The signum function used in the above expression for the moment, M_W, is defined as $signum(0) = 1$ and $signum(x) = x/|x|$. Finally, the parameter χ is the fraction of exposure of hoist cable to the rotor wake and is given approximately by

For $|\theta| \le \theta_{Lim}$

$$\chi \approx 1$$

For $|\theta| > \theta_{Lim}$

$$\chi \approx \frac{1}{\ell\sin|\theta|}\left[R + c(z_c - z)u(z_c - z) - signum(\theta)x_o\right]$$

Where

$$\theta_{Lim} = \text{acos}\left(\frac{-b_1 + \sqrt{b_1^2 - 4a_1c_1}}{2a_1}\right)$$

Given

$$a_1 \approx \ell^2\left(1 + c^2 u(z_c - \ell)\right)$$

$$b_1 \approx 2c\ell\left(R - signum(\theta)x_o\right)u(z_c - \ell) + 2c^2\ell(z_c - z_o)u(z_c - \ell)$$

$$c_1 \approx \left(R - signum(\theta)x_o\right)^2 - \ell^2 + 2c\left(R - signum(\theta)x_o\right)(z_c - z_o)u(z_c - \ell) + c^2(z_c - z_o)^2 u(z_c - \ell)$$

(5a-f)

In the above, the constant c is given by $c = 0.212$ and the function, $u(\ldots)$, is the Heaviside step function. The above expressions for the exposed (to the rotor wake) cable length are derived using simple trigonometric analysis while assuming that the rotor wake can be partitioned into two regions – one region where the wake boundary is approximately constant in radius, and the second region where the wake boundary is linear with respect to the axial coordinate, z.

Correspondingly, an effective vertical velocity can be used to define the cable effective vertical drag. This effective vertical velocity is defined in terms of the rotor wake momentum, which is constant and represented by the parameter J. The parameter J is given by the relationship $J = \rho A v_i^2 = k^2\rho A(T/2\rho A) = k^2 T/2$.

$$v_{ze} = \frac{\sqrt{J/\pi\rho}}{\left[R + c\left(z_c - (z_o - \ell)\right)u\left(z_c - (z_o - \ell)\right)\right]}$$

(6)

The vectored hoist "free-end" Cartesian and polar coordinates are given by

$$z = z_o - \ell\cos\theta$$

$$x = x_o + \ell\sin\theta$$

$$r = x/\cos\psi$$

(7a-c)

For the two-dimensional pendulum case, note that $\psi = 0$. In the above the cable is assumed to be rigid, i.e. doesn't "bow" under distributed aerodynamic loading. Further, it is assumed that the two different sets of loads for hoist hardware (for the when the hardware is mostly embedded within, or outside, the rotor wake) do not result in exhibition of bilinear cable characteristics (i.e. two different discrete cable displacement angles).

Correspondingly, the vertical and in-plane shear forces at the hoist winch/snubber (i.e. at the pendulum pivot). These in-plane and vertical shear forces applied to the helicopter airframe would then have to be countered by the pilot with rotor control inputs.

$$\begin{aligned}
&\Delta F_{in-plane} = \\
&-\sin(\varepsilon-\theta)\sum T_i \\
&+\frac{\ell}{g}\left(W_{rig} + W_{payload} + \frac{1}{2}W_{cable}\right)\left(\dot{\theta}\right)^2\sin\theta \\
&-\frac{1}{2}\rho\left(f_{x_{rig}} + f_{x_{payload}} + \frac{1}{4}f_{cable}\right)\left(\ell\dot{\theta}\right)^2 signum\left(\dot{\theta}\right)\cos\theta
\end{aligned}$$

$$\begin{aligned}
&\Delta F_{vert} = \\
&-\cos(\varepsilon-\theta)\sum T_i + W \\
&+\frac{\ell}{g}\left(W_{rig} + W_{payload} + \frac{1}{2}W_{cable}\right)\left(\dot{\theta}\right)^2\cos\theta \\
&+\frac{1}{2}\rho\left(f_{x_{rig}} + f_{x_{payload}} + \frac{1}{4}f_{cable}\right)\left(\ell\dot{\theta}\right)^2 signum\left(\dot{\theta}\right)\sin\theta \\
&+\frac{1}{2}\rho\left\{\left(f_{z_{rig}} + f_{z_{payload}}\right)v_z^2 + \frac{1}{2}\chi f_{cable}\, v_{ze}^2\cdot\sin^3|\theta|\right\}
\end{aligned}$$

(8a-b)

The above simple pendulum equations account for the both the inclusion of the influence of thrusters, aerodynamic damping both within and outside of the rotor wake, and the influence of vertical drag on the effective spring rate and dynamics of the pendulum motion.

Thruster Model

The sizing equations for the ducted fan thrusters are based upon earlier analysis/work derived in Ref. 15. These equations are simple first-order expressions that allow analysis of thrusters with circular and oval ducts as well as single, coaxial and tandem fans.

The static thrust characteristics of ducted-fans, including tandem dual-rotor fans in oval ducts, based upon the work of Ref. 15 is now considered. The "installed" static thrust, T, is given by Eq. 9a-c, where κ is the shroud thrust contribution (typically $\kappa \approx 0.3-0.4$), T_{UDF} is the un-ducted fan/rotor thrust (including interference effects if a multi-rotor configuration such as a coaxial or tandem fan/rotor system is employed), and $D_{screens}$ is the drag component reducing the net thrust by placing screens and/or other safeguards in the rotor wake for the protection of personnel and recovery victims.

$$T = (1+\kappa)T_{UDF} + D_{screens}$$

Where

$$D_{screens} \approx C_{D_{screens}}\cdot q_e A_e$$

And, expressing the effective dynamic pressure, q_e, in terms of an effective rotor wake induced velocity, v_e, the following approximate relationship applies

$$q_e = \frac{1}{2}\rho_e v_e^2 \approx \frac{T}{4A_e}$$

(9a-c)

Or, further,

$$D_{screens} \approx \left(C_{D_{screens}}/4\right)\cdot T$$

And so

$$T \approx \left(\frac{1+\kappa}{1-C_{D_{screens}}/4}\right)T_{UDF}$$

(10a-b)

The "static thrust" induced power of a ducted fan is (e.g. Ref. 16)

$$P_{DF} = \sqrt{\frac{T^3}{2\rho_e A_e}} \qquad (11)$$

The effective duct exit density and area, are given by ρ_e and A_e. For a low-pressure-ratio ducted fan: $\rho=\rho_e$ and $A_e=A_{DF}$. Note that for an "ideal" oval ducted fan $A_{DF} = \pi R^2 + 2sR$

References 17 and 18, for example, give the ratio of the induced power of an un-ducted tandem rotor configuration, with respect to an isolated rotor, as

$$\left.\frac{P_{UDF}}{P_I}\right|_{Induced\ power} = \left(\frac{2}{2-m}\right)^{1/2} \qquad (12a)$$

Where the dual-rotor overlap, m, is given by

$$m = \frac{2}{\pi}\left[\cos^{-1}\left(\frac{s}{2R}\right) - \left(\frac{s}{2R}\right)\sqrt{1-\left(\frac{s}{2R}\right)^2}\right] \qquad (12b)$$

And

$$P_I = \sqrt{\frac{T^3}{2\rho A}} \qquad A = \pi R^2 \qquad (12c\text{-}d)$$

Substituting the above equations into the ducted fan induced power expression, and solving for the power ratio P_{DF}/P_{UDF} gives

$$\left.\frac{P_{DF}}{P_{UDF}}\right|_{Induced\ Power} = \sqrt{\left(\frac{2-m}{2}\right)\left(\frac{\pi R^2}{A_{DF}}\right)} \qquad (13)$$

Now for a "real" oval ducted fan, introducing the ducted fan "efficiency," ε, the oval ducted fan effective exit area, A_{DF}, is given by the expression

$$A_{DF} = \left(\frac{2-m}{2}\right)\pi R^2 + \varepsilon\left[\left(\frac{2+m}{2}\right)\pi R^2 + 2sR\right] \qquad (14)$$

Note that when ε=1, the ideal oval ducted fan, then $A_{DF} = \pi R^2 + 2sR$, as noted earlier.

Substituting the expression for the effective ducted fan exit area into the induced power ratio equation yields an expression for the ratio of oval duct-fan induced power to un-ducted (tandem) fan induced power. This expression includes the introduction of a duct efficiency factor, ε, ($0 \le \varepsilon \le 1$). Ideal duct performance predicted when ε=1. When ε=0 the P_{DF}/P_{UDF} (induced power)=1 for all s/R values.

$$\left.\frac{P_{DF}}{P_{UDF}}\right|_{Induced\ Power} = \sqrt{\frac{2-m}{\left[(2-m)+(2+m)\varepsilon + \frac{4\varepsilon s}{\pi R}\right]}} \qquad (15)$$

Where m, the rotor overlap, is given by Eq. 12b and the duct efficiency, ε, is an empirical constant. Though the duct efficiency, ε, is treated as invariant with respect to s/R changes in the predictions in this paper, it probably does in actuality vary with s/R to some degree.

The above discussion for ducted fan performance is for static thrust conditions. The above performance equations are therefore applicable for when the vectored rescue hoist, with ducted fan thrusters, is outside the rotor wake slipstream. When the hoist is within the rotor wake slipstream, the ducted fans are in significant cross-flow conditions. However, the experimental work of Ref. 12 would suggest that when ducted fan axis is approximately normal to the cross-flow induced by the rotor wake, the ratio of ducted fan thrust to power is approximately constant, or even slightly increases, with increasing cross-flow velocity, as compared to the ducted fan static fan performance. For ducted fan incidence angles significantly less than the ninety degrees, i.e. $\varepsilon << \pi/2$ or rather as $\varepsilon \to 0$, the ducted fan thrust decreases substantially as predicted by momentum theory. This is fortunate as it implies that static thrust sizing of the ducted fan thrusters under no-cross-flow conditions should yield reasonable sizing estimates.

Nonetheless, the ducted-fan axial flow momentum theory analysis can be modified to account for cross-flow in the following manner.

$$T_{hoist} = T + \Delta T_{crossflow} \tag{16}$$

$$P_{hoist} = P_{DF} + \Delta P_{crossflow} + \Delta P_{swing}$$

$$\Delta P_{crossflow} = \dot{m}_{DF} v_z^2 \sin(\varepsilon - \theta) = \sqrt{\frac{\rho A_{DF} T}{2}} \cdot v_z^2 \sin(\varepsilon - \theta)$$

$$\Delta P_{swing} = T\ell\dot{\theta} \cdot \sin\varepsilon \tag{17a-c}$$

Where $\Delta T_{crossflow}$ is the ducted fan's "shroud lift" contribution in "cross flow." This "shroud lift" has been predicted in Ref. 19 and inferred from the experimental work of Ref. 12. There is no simple analysis to predict the shroud lift contribution in cross-flow. Therefore, for the sake of sizing conservatism the $\Delta T_{crossflow}$ contribution to the vectored hoist thruster performance has not been included in the analysis results presented in this paper. The parameter $\Delta P_{crossflow}$ is the incremental power increase for the "ram drag" effect noted in Ref. 20. (Alternatively, this effect is also referred to as "momentum drag" in Ref. 21.) This incremental power increase, $\Delta P_{crossflow}$, is due to the ducted fan thruster in cross flow having to redirect freestream flow over the ducted fan inlet to align it with the duct axis. For conservatism, the "ram drag" incremental power increase is included in the sizing analysis. On the other hand, because of its comparatively small magnitude, the "ram drag" effect's slight counterbalancing effect on cable tension is not taken into account in this paper's ducted fan sizing analysis. Finally, the parameter ΔP_{swing} incremental power contribution stems from the nonzero freestream axial flow induced power (a.k.a. "climb" power from conventional rotary-wing aerodynamic theory, e.g. Ref. 18) required by the ducted fan thrusters during the hoist's pendulum motion, or rather "swing".

Rotor Wake Modeling

Unlike other helicopter slung load analyses, e.g. Refs. 22-25, the "vectored" hoist rig and cabling is not always embedded in the rotor wake.

The mean rotor wake velocities for the near- and mid-field are derived from actuator disk vortex theory, see, for example, Refs. 18 and 26. Using the nomenclature, and expressions, from Ref. 26 for the single main rotor case versus the complete side-by-side rotor case originally considered in Ref. 26, the following equations are used to define all three components of the near- and mid-field rotor wake mean velocities.

$$\vec{v}_R = v_x \vec{i}_* + v_y \vec{j}_* + v_z \vec{k}_* \tag{18}$$

Or, specifically,

$$\vec{v}_R = \left\{ \frac{\Gamma}{4\pi} I_{RR} - \frac{\gamma}{4\pi} I_R \right\} \vec{i}_* + \left\{ \frac{\Gamma}{4\pi} J_{RR} - \frac{\gamma}{4\pi} J_R \right\} \vec{j}_* - \frac{\gamma}{4\pi} (K_R) \vec{k}_* \tag{19}$$

Where, in the above, an approximate rotor wake model is defined using the following induced terms (defined in terms of the polar coordinates r, z, and ψ). This approximate model incorporates aspects of classic actuator disk vortex theory (induced velocity axial distribution by means of the solution for a constant diameter vortex cylinder), mass flow continuity (approximately defining the rotor wake slipstream boundary by means of mass flow continuity using the previously mentioned induced velocity axial distribution), and wake non-uniformity in terms of the induced velocity radial distribution (defined using the Prandtl lightly loaded rotor in hover tip loss solution). Note that the swirl contributions are based upon work noted in Ref. 26.

$$K_R = 4\left\{\frac{z}{\sqrt{R^2+z^2}}-1\right\}\text{acos}\left(e^{\frac{(r-R_S(z))u(R_S(z)-r)N}{R\sqrt{2C_T}}}\right)$$

Where the near-field rotor wake slipstream boundary is defined by

$$R_S(z) = R\cdot\left(1-\frac{z}{\sqrt{R^2+z^2}}\right)^{-1/2}$$

Further

$$J_R = \frac{(r+R)\cos\psi}{r(1+|z|)}\cdot\left\{2\,\text{E}\left(\frac{\pi}{2},\frac{2\sqrt{rR}}{r+R}\right)-\left[1+\left(\frac{r-R}{r+R}\right)^2\right]\text{F}\left(\frac{\pi}{2},\frac{2\sqrt{rR}}{r+R}\right)\right\}$$

$$I_R = \frac{(r+R)\sin\psi}{r(1+|z|)}\cdot\left\{\left[1+\left(\frac{r-R}{r+R}\right)^2\right]\text{F}\left(\frac{\pi}{2},\frac{2\sqrt{rR}}{r+R}\right)-2\,\text{E}\left(\frac{\pi}{2},\frac{2\sqrt{rR}}{r+R}\right)\right\}$$

$$I_{RR} = \frac{r\cos\psi}{r^2+a^2}\left[1-\frac{z}{\sqrt{r^2+z^2}}\right]$$

$$J_{RR} = \frac{r\sin\psi}{r^2+a^2}\left[1-\frac{z}{\sqrt{r^2+z^2}}\right]$$

(20a-e)

Where in the above in terms of complete elliptic integrals of the first and second kind, $\text{F}(\pi/2,k)$ and $\text{E}(\pi/2,k)$. The parameter a is incorporated in the I_{RR} and J_{RR} expressions to avoid singularities in the rotor wake swirl velocity components.

In the rotor far-wake a jet-like velocity profile is assumed. The far-wake axial velocity profile used in this study is given by Eq. 21a-b; Eq. 21a-b is based upon classic viscous turbulent circular jet work from Görtler, see e.g. Refs. 27-29.

$$\vec{v}_R = 0\vec{i}_* + 0\vec{j}_* + \left\{v_{z_{\max}}\left(1+\eta^2/4\right)^{-2}\right\}\vec{k}_*$$

Where

$$\eta = \sigma\frac{r}{z}$$

(21a-b)

Note that the constant $\sigma \approx 15.2$ based upon circular jet profile matching with experimental data.

A simple nondimensional axial coordinate cutoff distance is defined, z_c/R; this cutoff distance partitions the rotor wake into near-field, transition, and far-field "jet flow" regions. Note that the parameter k_c defines the fraction of axial velocity attained as the theoretical momentum theory asymptotic far-wake value; for the analysis performed in this paper, $k_c = 0.99$.

$$z_c/R = (1-2k_c)\Big/\sqrt{1-(1-2k_c)^2}$$

Or

$$z_c/R \approx -5$$

(22a-b)

The rotor wake transition from the velocities defined by Eq. 20a-e to those defined by Eq. 21a-b is modeled by the following expression (for $z \le z_c$)

$$\vec{v}_R\big|_{Transition} = \left(e^{a(z-z_c)/R}\right)\vec{v}_R\big|_{Near-Field} + \left(1-e^{a(z-z_c)/R}\right)\vec{v}_R\big|_{Far-Field}$$

(23)

Where the constant a can be semi-empirically assigned; for the work described in this paper, the constant has be somewhat arbitrarily assigned as $a = 1$).

Note that "transitioning" between flow solutions for two semi-discrete regions of flow, can be accomplished in general in the following manner. For two flow regions, and corresponding solutions, where $J = constant$, it follows that the intermediate "transition" region, described by a transition expression incorporating the two discrete regions/solutions with respect to a general coordinate, q, must as well preserve the requirement that the total momentum in this transition region is also constant. This is accomplished by expressing a transition expression (employing a function $f(q)$ in terms of the general coordinate, q) of the following general form. I.e.

$$V|_{Transition} = f(q)V|_{Region\ \#1} + \left(1 - f(q)\right)V|_{Region\ \#2} \tag{24}$$

Transition functions of this form can be proven to be valid as follows. As momentum in the transition region must be constant the following must be true

$$\int_{-\infty}^{\infty} \rho V dA|_{Transition} = J = constant \tag{25}$$

Substitution the transition expression into the above gives

$$\begin{aligned}\int_{-\infty}^{\infty} \rho V dA|_{Transition} &= f(q)\int_{-\infty}^{\infty} \rho V dA|_{Region\ \#1} \\ &\quad + \left(1 - f(q)\right)\int_{-\infty}^{\infty} \rho V dA|_{Region\ \#2} \\ &= J\end{aligned} \tag{26}$$

Now, having previously established, the following

$$\int_{-\infty}^{\infty} \rho V dA|_{Region\ \#1} = J$$

And

$$\int_{-\infty}^{\infty} \rho V dA|_{Region\ \#2} = J \tag{27a-b}$$

Therefore, it must hold true that this general transition function also preserves constant momentum

$$\int_{-\infty}^{\infty} \rho V dA|_{Transition} = f(q)J + \left(1 - f(q)\right)J = J \tag{28}$$

The general transition function, $f(q)$, is subject to (by definition) the following constraints.

$$f(q) \to 1 \qquad \text{As} \qquad q \to Region\ \#1$$

$$f(q) \to 0 \qquad \text{As} \qquad q \to Region\ \#2 \tag{29a-b}$$

Other constraints necessary to define a specific transition function are dependent upon the particular flow problem being studied. In defining the hover rotor wake transition flow model employed in this paper, an ad hoc approach was taken to define

$$f(q) \Rightarrow e^{a(z_c - z)/R} \tag{30}$$

Matching the rotor wake momentum from the actuator disk model with the jet flow momentum expression gives

$$J = k^2 T_R / 2$$

And

$$v_{z_{\max}} = \frac{1}{b}\sqrt{\frac{J}{\rho}} \tag{31a-b}$$

Where J is the wake/jet momentum, which is constant; the parameter T_R is the helicopter main rotor thrust for the given rotor wake. From classic jet flow theory $-b/z \approx c = 0.212$.